MDPI

Article

Performance Analysis for In-band Full-duplex Non-Orthogonal Multiple Access Relaying System With Channel Estimation Errors and Low-resolution ADCs

Siye Wang [1,†]*, Yong Yang [2,†], Yeqin Huang [†] and Wenbo Xu[†]

† School of Arificial Intelligence, Beijing University of Posts and Telecommunications
[1] wsy@bupt.edu.cn
[2] YangYong.cn@outlook.com
* Correspondence: wsy@bupt.edu.cn.
† Current address: 10 Xitucheng Rd., Haidian District, Beijing, 100876 CHINA.

Abstract: In this paper, we analyze the ergodic rates and outage probability of in-band full-duplex (IBFD) cooperative non-orthogonal multiple access (C-NOMA) system with amplify-and-forward (AF) protocol in the presence of channel estimation errors and quantization noise in low-resolution analog to digital converters (ADCs). The loopback interference in IBFD transceivers also impacts the system performance. We derive the closed-form and accurate approximation expressions for the outage probability **and** the ergodic rate, respectively. Monte Carlo simulations verify the validity of theoretical results. Simulation results show that system performance is more sensitive to the signal-to-noise ratio, loopback interference, and channel estimation error levels than the quantization bits. When the quantization bits are sufficient, the system performance is no different from an ideal ADCs system.

Keywords: full-duplex; cooperative communication; non-orthogonal multiple access; channel estimation errors; low-resolution ADCs

Citation: Wang, S.; Yong, Y.; Yeqin, H.; Wenbo Xu. Performance Analysis for In-band Full-duplex Non-Orthogonal Multiple Access Relaying System With Channel Estimation Errors and Low-resolution ADCs. *Appl. Sci.* **2022**, *1*, 0. https://doi.org/

Received:
Accepted:
Published:

1. Introduction

With the rapid development of 5G/6G technology, mobile communication systems need to adapt to more complicated communication requirements, including high mobility, higher throughput, enhanced coverage, **lower** latency, and massive connectivity. Non-Orthogonal Multiple Access (NOMA) has recently received significant attention due to its potential to increase spectral efficiency, reduce latency, achieve enhanced user fairness, **enlarge** connections, and **promote** diverse quality of service (QoS) [1]. Different from the previous orthogonal multiple access (OMA) schemes such as Frequency-Division Multiple Access (FDMA), Time-Division Multiple Access (TDMA), Code-Division Multiple Access (CDMA), and Orthogonal Frequency Division Multiple Access (OFDMA), NOMA can serve more users than available resources in either of the power-domain (PD-NOMA) and code-domain (CD-NOMA) at the cost of increased receiver complexity [2]. ~~In the~~ Meanwhile, relay cooperation can enhance wireless coverage and improve ~~the~~ communication reliability. There are two common processing protocols for relaying signals~~, namely~~: amplify-and-forward (AF) and decode-and-forward (DF). Cooperative Non-Orthogonal Multiple Access (C-NOMA) has attracted great attention since combining cooperative relay **with** NOMA can further improve diversity gain and transmission efficiency[3–5].

In traditional wireless communication scenarios, time or frequency resources are adopted to support duplex transmission, known as half-duplex or out-of-band full-duplex. However, recently, in-band full-duplex (IBFD) radio was proposed as a promising technique for the **next-generation** wireless communication systems, since it has the potential to double the spectrum efficiency by enabling wireless terminals to transmit and receive

simultaneously over the same carrier frequency band [6–9]. However, the loopback interference (LI) leaked from the transmit antenna to the receive antenna is a challenge in the IBFD communication system. It increases the complexity of the system design and limits the performance of the IBFD system. Antenna isolation designs can achieve LI cancellation of 20-45 dB, while novel RF cancellation can yield LI cancellation of nearly 25-45 dB. Analog and digital cancellation can cancel the remaining LI. However, due to the nonlinear imperfections introduced by RF devices, the residual LI still exists even with these cancellation methods. With the gradual development and continuous improvement of antenna-domain, analog-domain and digital-domain combined interference mitigation techniques, the benefits of the IBFD mode of operation are getting closer to realization. Thus, the research area of IBFD relaying CNOMA has attracted great attention since it can further improve system performance [10–13] .

带内双工、**LI**消除

NOMA的原理**,** 功率域和编码域**NOMA**。

In general, non-orthogonal multiple access techniques include two types, power-domain multiplexing, and code-domain multiplexing. In code-domain multiplexing, each user exploit different codes and use the same time-frequency resources. Although code-domain NOMA has a better performance than power-domain NOMA, it requires a high bandwidth and it cannot be easily applied to the current communication systems[14]. Clearly, power-domain NOMA has a simple implementation. For simplicity, We shall only discuss the power-domain NOMA in this paper. In power-domain multiplexing, each user exploit a power coefficient according to its channel condition. At the transmitter side, all the information signals of multiple users are superimposed. The receiver side applies the successive interference cancellation(SIC)[15]. The users decodes the signals one by one until the desired user's signal is obtained.

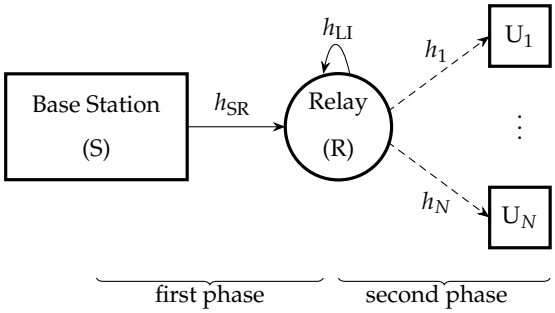

Figure 1. System model of cooperative-NOMA relaying system without direct link.

协作**-NOMA,** 直径**/Not**

In cooperative communications, one or multiple relays help the transmission between the source and destination. There are two common processing methods for relaying signals, amplify-and-forward (AF) and decode-and-forward (DF). Moreover, the relaying mode can be categorized as half-duplex(HD) and full-duplex(FD). Full-duplex transceiver process the date reception and transmission simultaneously in the same frequency band and time slot. In words, the combination of NOMA and cooperative communication has been considered a solution to enhance the system efficiency. Generally, there are two scenarios of cooperative NOMA systems. In [16], the authors proposed the scheme which coordinated direct and relay transmission is considered. Differ from [16], in [17], authors proposed a cooperative relaying system in figure 1. Figure 1 shows a cooperative scheme without direct link. In figure 1, $\mathrm{U}_1, \cdots, \mathrm{U}_N$ are N users in the downlink network. To get exact expressions related to achievable system performance, authors in [17] derived in i.i.d. Rayleigh fading channels.

低精度**ADCs**

Limited by antenna design and RF cancellation, it is difficult to fully mitigate LI before the signal is fed into the analog to digital converters (ADCs). ADC is an indispensable component in practical communication systems, and the financial budget limits its resolution. On the other hand, low-resolution ADCs cause ~~the~~ quantization error, which also has **an** impact on the communication performance of the practical system. The input signal of the ADC is usually composed of the desired signal, the interference signal, and

the noise, which means that the interference signal and the noise occupy a wide dynamic range. Specifically, power consumption and chip area of ADCs grow exponentially with the number of quantization bits. Recently, the IBFD systems analysis considering the problems arising from the quantization of low-resolution ADCs **is** investigated [18–20].

信道估计误差

In practical communication scenarios, the wireless channel state information (CSI) may only be partially known at the receiver, and ~~**in order**~~ to acquire such knowledge, channel estimation must be performed through training pilots. **In various studies, channel estimation is done by least squares(LS) estimator, minimum mean square error(MMSE) estimator and even deep learning methods**[21]. The Doppler shift and noise on the pilot signals could produce ~~**the**~~ channel estimation errors, which is another main reason for performance degradation in wireless networks. Several works have investigated the effect of channel uncertainty in relay cooperative systems.

In the existing related researches on the performance analysis of IBFD Cooperative-NOMA, such as [16,17,22–24], some authors use ideal RF models, while others consider the I/Q imbalance and imperfect SIC. But none of them consider the performance impact brought by the resolution of the ADCs and the error of the channel estimation.

As pointed out in the previous discussion, loopback interference, quantization errors of ADCs and channel estimation errors will all have a certain impact on the NOMA relaying network. This paper will analyze the system performance in the presence of these real-world non-ideal factors, including outage probability and ergodic rate. The contributions of this letter are as follows:

1. We consider a full-duplex Cooperative-NOMA wireless communication system, which uses relays to amplify and forward signals to realize signal transmission between base stations and terminals. Two non-ideal conditions, channel estimation error, and low-precision ADCs are considered in our model.
2. We derived general expressions for the system ergodic rate and outage probability.
3. We verified our mathematical results via Monte Carlo simulations. For the C-NOMA relaying network, we discussed the impact of base station transmission power, relay amplification, and forwarding power, relay loopback self-interference level, quantization error level, and channel estimation error level on the system performance. Theoretical and simulation results demonstrate the feasibility of the proposed theoretical method.

We organize the rest of this paper as follows: Section II introduces the system model of the multi-user C-NOMA relaying network and signal model of low-resolution ADCs and channel estimation errors. Section III and IV deduce and analyze the theoretical results of system ergodic rate and outage probability, respectively. Section V shows the theoretical results and simulation results of the system performance index under different parameters. Finally, section VI is a conclusion of the full text.

Notations: We use $\mathcal{CN}$ to denote the complex normal distribution and i.i.d. to denote "independent and identically distributed". $\mathbb{E}(\cdot)$ and $\Pr(\cdot)$ denotes the expected value of random variables and probability of events, respectively.

2. System Model

In this paper, we consider the system model in figure 1, which is an IBFD C-NOMA relaying network consisting of one base station (S), one IBFD relay(R), and N user equipments (UEs). In this network, both the base station and each UE are equipped with a single antenna, while the relay has one transmit and one receive antenna.

We suppose that all the channels in figure 1 are Rayleigh fading, and channel estimation errors exist. There is no direct link exists between the BS and UEs due to the distance and the path fading. We have also considered the impact of low-resolution ADCs on every user node. Based on NOMA protocol, we rearrange the N users according to the estimate of channel gains in the second phase. Let $(\hat{h}_1, \cdots, \hat{h}_N)$ denote the order statistic of $(\hat{h}_{\mathrm{RU}_1}, \cdots, \hat{h}_{\mathrm{RU}_N})$ in modulus, namely, $|\hat{h}_n|$ is the nth-smallest value in $\{|\hat{h}_{\mathrm{RU}_1}|, \cdots, |\hat{h}_{\mathrm{RU}_N}|\}$.

Then we have $|\hat{h}_1| \leq \cdots \leq |\hat{h}_N|$. Here and in what follows, we shall denote the user corresponding to $\hat{h}_n$ by nth user or user n ($n \in [N]$).

发送端发信号。

In the first phase, the superimposed signal

$$s_{\mathrm{S}} = \sqrt{P_{\mathrm{S}}} \sum_{n=1}^{N} \sqrt{a_n} x_n \tag{1}$$

is transmitted from the base station, where P_{S} is the transmission power at the base station S, a_n is the power allocation coefficient for user n and x_n are the information signals transmitted to user n with unit energy, i.e., $\mathbb{E}|x_n|^2 = 1$, $n \in [N]$. The power coefficients are subjected to $\sum_{n=1}^{N} a_n = 1$ and $a_1 \geq \cdots \geq a_N$.

The received signal at relay R can be expressed as

$$r_{\mathrm{R}} = h_{\mathrm{SR}} s_{\mathrm{S}} + h_{\mathrm{LI}} s_{\mathrm{R}} + w_{\mathrm{R}}, \tag{2}$$

where $w_{\mathrm{R}} \sim \mathcal{CN}(0, \sigma_{\mathrm{R}}^2)$ denotes the complex circularly-symmetric additive white Gaussian noise (AWGN), $h_{\mathrm{LI}} \sim \mathcal{CN}(0, \beta_{\mathrm{R}})$ is the residual loop back interference coefficient after some cancellation methods.

经过带有估计误差的信道。

We use the channel estimation model of block fading in [19], which assume that all the channel are quasi-static Rayleigh fading. Namely, all the channels are assumed to be block Rayleigh fading, i.e., the channel coefficients is constant on a block, and it only change between blocks and blocks. Each channel coefficient h is a sum of its estimate and the estimation error

$$h = \hat{h} + \epsilon_h, \tag{3}$$

where $\hat{h}$ is the estimate of the channel coefficient h and ϵ_h is the corresponding estimation error. The model assume that $\hat{h} \sim \mathcal{CN}(0, \sigma_{\hat{h}}^2)$ and $\epsilon_h \sim \mathcal{CN}(0, \sigma_{\epsilon_h}^2)$ and the channel estimate and estimation error are uncorrelated.

Let $h_{\mathrm{SR}} \sim \mathcal{CN}(0, \tilde{\beta}_{\mathrm{SR}})$ denote the channel coefficient from S to R and $h_{\mathrm{RU}_1}, \cdots, h_{\mathrm{RU}_N} \overset{\text{i.i.d}}{\sim} \mathcal{CN}(0, \tilde{\beta}_{\mathrm{RU}})$ denote the channel coefficients between R and N users. Then we have

$$h_{\mathrm{SR}} = \hat{h}_{\mathrm{SR}} + \epsilon_{\mathrm{SR}}, \; h_{\mathrm{RU}_n} = \hat{h}_{\mathrm{RU}_n} + \epsilon_{\mathrm{RU}_n}, \tag{4}$$

where channel estimation error term $\epsilon_{\mathrm{SR}} \sim \mathcal{CN}(0, \sigma_{\mathrm{SR}}^2)$ and $\epsilon_{\mathrm{RU}_1}, \cdots, \epsilon_{\mathrm{RU}_N} \overset{\text{i.i.d}}{\sim} \mathcal{CN}(0, \sigma_{\mathrm{RU}}^2)$. So the channel estimates $\hat{h}_{\mathrm{SR}} \sim \mathcal{CN}(0, \beta_{\mathrm{SR}} = \tilde{\beta}_{\mathrm{SR}} - \sigma_{\mathrm{SR}}^2)$ and $\hat{h}_{\mathrm{RU}_1}, \cdots, \hat{h}_{\mathrm{RU}_N} \overset{\text{i.i.d}}{\sim} \mathcal{CN}(0, \beta_{\mathrm{RU}} = \tilde{\beta}_{\mathrm{RU}} - \sigma_{\mathrm{RU}}^2)$. Here, we assume that the variables above in the first and second phases are mutually uncorrelated.

确定放大转发的增益系数。

By the AF protocol, the relay amplifies the received signal by a factor A_{R} with a processing delay τ. The transmit signal s_{R} of the relay can be expressed as

$$s_{\mathrm{R}}[n] = \sqrt{P_{\mathrm{R}}} A_{\mathrm{R}} r_{\mathrm{R}}[n - \tau], \tag{5}$$

where P_{R} is the transmit power of the relay. Since the instantaneous transmit power of R should be P_{R}, i.e.,

$$\begin{aligned} P_{\mathrm{R}} = \mathbb{E}|s_{\mathrm{R}}|^2 &= P_{\mathrm{R}} A_{\mathrm{R}}^2 \mathbb{E}|r_{\mathrm{R}}|^2 \\ &= P_{\mathrm{R}} A_{\mathrm{R}}^2 \left[\mathbb{E}|h_{\mathrm{SR}}|^2 P_{\mathrm{S}} + \beta_R P_{\mathrm{R}} + \sigma_{\mathrm{R}}^2 \right]. \end{aligned} \tag{6}$$

Hence, the amplification factor can be given as

$$A_{\mathrm{R}} = \frac{1}{\sqrt{P_{\mathrm{S}} |\hat{h}_{\mathrm{SR}}|^2 + P_{\mathrm{S}} \sigma_{\mathrm{SR}}^2 + P_{\mathrm{R}} \beta_{\mathrm{R}} + \sigma_{\mathrm{R}}^2}}. \tag{7}$$

In the second phase, after the relay R applies AF protocol, the signal s_R transmit from R to user $U_1, \cdots, U_N$. The received signal at user U_n can be expressed as

$$r_n = h_n s_R + w_n, \tag{8}$$

where $w_n \sim \mathcal{CN}(0, \sigma_U^2)$ denotes the AWGN at user n.

After the quantization, users get the output of the ADCs. As described in [19], the output of a low-resolution ADC corresponding to input $r_n(m)$ can be expressed as

在接收端的量化。

$$\bar{r}_n(m) = \alpha r_n(m) + \bar{n}_r, \tag{9}$$

where the values of α is determined by the quantization bits of the ADC and $\bar{n}_r$ denotes the additive quantization noise.

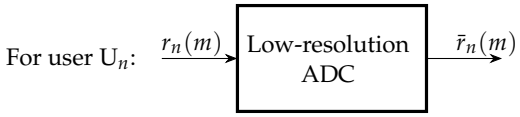

Figure 2. System model of low-resolution ADCs.

Let b be the number of quantization bits. When $b > 5$, the parameter α is given by

$$\alpha = 1 - \frac{\pi\sqrt{3}}{2} 2^{-2b}, \tag{10}$$

When quantization bits $b \leq 5$, the value of α is given as follows:

quantization bits	1	2	3	4	5
α	0.6366	0.8825	0.96546	0.990503	0.997501

Moreover, the quantization noise term $\bar{n}_r$ has a complex normal distribution with zero mean and variance

$$\mathbb{E}|\bar{n}_r|^2 = \alpha(1-\alpha)\mathbb{E}|r_n(m)|^2. \tag{11}$$

In other words, the power of quantized signal obtained by the user n can be expressed as

$$\begin{aligned} \mathbb{E}|\bar{r}_n|^2 &= \mathbb{E}|\alpha r_n|^2 + \mathbb{E}|\bar{w}_n|^2 \\ &= \alpha^2 \mathbb{E}|r_n|^2 + \alpha(1-\alpha)\mathbb{E}|r_n|^2 \\ &= \alpha \mathbb{E}|r_n|^2. \end{aligned} \tag{12}$$

To sum up, the quantized signal obtained by the user n is given by

$$\begin{aligned} \bar{r}_n &= \alpha r_n + \bar{n}_r \\ &= \alpha(h_n s_R + w_n) + \bar{n}_r \\ &= \alpha(h_n \sqrt{P_R} A_R r_R + w_n) + \bar{n}_r \\ &= \alpha[h_n \sqrt{P_R} A_R (h_{SR} s_S + h_{LI} s_R + w_R) + w_n] + \bar{n}_r \\ &= \alpha\left[(\hat{h}_n + \epsilon_n)\sqrt{P_R} A_R \left((\hat{h}_{SR} + \epsilon_{SR}) s_S + h_{LI} s_R + w_R\right) + w_n\right] + \bar{n}_r \\ &= \alpha\left[(\hat{h}_n + \epsilon_n)\sqrt{P_R} A_R \left((\hat{h}_{SR} + \epsilon_{SR})\left(\sqrt{P_S}\sum_{n=1}^{N}\sqrt{a_n} x_n\right) + h_{LI} s_R + w_R\right) + w_n\right] + \bar{n}_r. \end{aligned} \tag{13}$$

Based on the NOMA concept, the users need to perform successive interference cancellation(SIC) processes. The instantaneous signal-to-interference-plus-noise ratio(SINR) of ith user to decode jth user's signal($j \leq i$) can be expressed as

$$\begin{aligned}\mathrm{SINR}_{i,j} &= \alpha^2|\hat{h}_i|^2 A_{\mathrm{R}}^2 P_{\mathrm{R}}|\hat{h}_{\mathrm{SR}}|^2 P_{\mathrm{S}} a_j \\ &\cdot \Big(\alpha(|\hat{h}_i|^2+\sigma_{\mathrm{RU}}^2)A_{\mathrm{R}}^2 P_{\mathrm{R}}(|\hat{h}_{\mathrm{SR}}|^2+\sigma_{\mathrm{SR}}^2)P_{\mathrm{S}} \\ &- \alpha^2|\hat{h}_i|^2 A_{\mathrm{R}}^2 P_{\mathrm{R}}|\hat{h}_{\mathrm{SR}}|^2 P_{\mathrm{S}} \sum_{u=1}^{j} a_u \\ &+ \alpha(|\hat{h}_i|^2+\sigma_{\mathrm{RU}}^2)A_{\mathrm{R}}^2 P_{\mathrm{R}}(\ell_{\mathrm{R}} P_{\mathrm{R}}+\sigma_{\mathrm{R}}^2)+\alpha\sigma^2\Big)^{-1}.\end{aligned} \tag{14}$$

Here, for user j, the signals to user $\{j+1,\cdots,N\}$ are treated as the multiple access interference signals. We subtract only the power of the signals to user $\{1,\cdots,j\}$ from the total power in the denominator.

To make things easier to write, we set $\gamma_1 = P_{\mathrm{S}}/\sigma_{\mathrm{R}}^2$, $\gamma_2 = P_{\mathrm{R}}/\sigma_{\mathrm{U}}^2$, $\gamma_3 = \beta_{\mathrm{R}} P_{\mathrm{R}}/\sigma_{\mathrm{R}}^2$, $\Gamma_1 = \gamma_1\gamma_2$, $\Gamma_2 = \gamma_2(\sigma_{\mathrm{SR}}^2\gamma_1+\gamma_3+1)$, $\Gamma_3 = \gamma_1(\gamma_2\sigma_{\mathrm{RU}}^2+1)$, $\Gamma_4 = (\sigma_{\mathrm{RU}}^2\gamma_2+1)(\sigma_{\mathrm{SR}}^2\gamma_1+\gamma_3+1)$ and $b_j = (1-\alpha\sum_{u=1}^{j} a_u)$. Now it follows that

$$\mathrm{SINR}_{i,j} = \frac{\alpha a_j \Gamma_1|\hat{h}_i|^2|\hat{h}_{\mathrm{SR}}|^2}{b_j\Gamma_1|\hat{h}_i|^2|\hat{h}_{\mathrm{SR}}|^2+\Gamma_2|\hat{h}_i|^2+\Gamma_3|\hat{h}_{\mathrm{SR}}|^2+\Gamma_4}. \tag{15}$$

3. Ergodic Rates Analysis

After finding SINR expressions of each user, the ergodic rates analysis can be done. Although there is no closed-form expressions for this problem, we can easily get an accurate approximation. The expression for the ergodic rates(ER) for user n is expressed as

$$C_n = \mathbb{E}\log_2(1+\mathrm{SINR}_{n,n}), \quad n \in [N] \tag{16}$$

Theorem 1. *The expression for the ergodic rates for user n can be derived as*

$$\begin{aligned}C_n \approx &\sum_{s=0}^{n-1} \frac{N!(-)^s(N-n+s+1)^{-1}}{(n-1)!(N-n)!\ln 2}\binom{n-1}{s} \\ &\cdot\left[I\Big(\frac{\theta_{n,2}}{\theta_{n,1}},\frac{\theta_{n,3}}{\theta_{n,1}},\frac{\theta_{n,4}}{\theta_{n,1}}\Big)-I\Big(\frac{\theta_{n,2}}{\tilde{\theta}_{n,1}},\frac{\theta_{n,3}}{\tilde{\theta}_{n,1}},\frac{\theta_{n,4}}{\tilde{\theta}_{n,1}}\Big)\right],\end{aligned} \tag{17}$$

where $\theta_{n,1} = (b_n+\alpha a_n)\Gamma_1\beta_{\mathrm{RU}}\beta_{\mathrm{SR}}$, $\tilde{\theta}_{n,1} = b_n\Gamma_1\beta_{\mathrm{RU}}\beta_{\mathrm{SR}}$, $\theta_{n,2} = \beta_{\mathrm{RU}}\Gamma_2$, $\theta_{n,3} = \beta_{\mathrm{SR}}\Gamma_3(N-n+s+1)$ *and* $\theta_{n,4} = \Gamma_4(N-n+s+1)$. *The function* $I(\cdot,\cdot,\cdot)$ *in* (17) *is given by*

$$\begin{aligned}I(p,q,r) \approx &\,\mathrm{e}^{\frac{r}{q}}E_1\Big(\frac{r}{q}\Big)+\mathrm{e}^{q}E_1(q) \\ &+\mathrm{e}^{p}E_1(p)\sum_{\lambda\in\Lambda}h_\lambda\mathrm{e}^{-k_\lambda q}\Big(\frac{x_\lambda^2}{2}+\sqrt{x_\lambda}J_1(-2\sqrt{x_\lambda})\Big) \\ &+\sum_{\lambda\in\Lambda}h_\lambda\mathrm{e}^{-k_\lambda q}\left[\frac{x^2}{2p}-\sum_{v=2}^{V}\sum_{u=1}^{v-1}\frac{(u-1)!(-)^{v-u}x^v}{v!(v-1)!p^u}\right],\end{aligned} \tag{18}$$

where Λ, h_λ, k_λ *are defined in* (23), $x_\lambda = k_\lambda(pq-r)$, $J_1(\cdot)$ *denotes the* 1*st-order Bessel function of the first kind.*

Proof. From the knowledge of order statistic[25], it is easy to see that $|\hat{h}_n|^2$ has a density function

$$\begin{aligned} f_n(x) &= \frac{N!\beta_{\mathrm{RU}}^{-1}}{(n-1)!(N-n)!}(\mathrm{e}^{-\frac{1}{\beta_{\mathrm{RU}}}x})^{N-n+1}\left(1-\mathrm{e}^{-\frac{1}{\beta_{\mathrm{RU}}}x}\right)^{n-1} \\ &= \frac{N!\beta_{\mathrm{RU}}^{-1}}{(n-1)!(N-n)!}\sum_{s=0}^{n-1}\binom{n-1}{s}(-)^s\mathrm{e}^{-\frac{N-n+s+1}{\beta_{\mathrm{RU}}}x}\mathbf{1}_{(x\geq 0)}, \end{aligned} \tag{19}$$

where $\mathbf{1}_{(\cdot)}$ denotes the indicator function. Using (15), (16), 19, we get

$$\begin{aligned} C_n = \int_0^\infty\int_0^\infty \log_2\left(1+\frac{\alpha a_n\Gamma_1 xy}{b_n\Gamma_1 xy+\Gamma_2 x+\Gamma_3 y+\Gamma_4}\right) \\ f_n(x)\beta_{\mathrm{SR}}^{-1}\mathrm{e}^{-\frac{1}{\beta_{\mathrm{SR}}}y}\,\mathrm{d}x\mathrm{d}y. \end{aligned} \tag{20}$$

Changing variable $x \mapsto (N-n+s+1)\beta_{\mathrm{RU}}^{-1}x$ and $y \mapsto \beta_{\mathrm{SR}}^{-1}y$ gives

$$\begin{aligned} C_n = \sum_{s=0}^{n-1}\frac{N!(-)^s(N-n+s+1)^{-1}}{(n-1)!(N-n)!\ln 2}\binom{n-1}{s} \\ \cdot\int_0^\infty\int_0^\infty \ln\left(\frac{\theta_{n,1}xy+\theta_{n,2}x+\theta_{n,3}y+\theta_{n,4}}{\tilde{\theta}_{n,1}xy+\theta_{n,2}x+\theta_{n,3}y+\theta_{n,4}}\right)\mathrm{e}^{-x-y}\,\mathrm{d}x\mathrm{d}y. \end{aligned} \tag{21}$$

We could carry on calculating the integral in (21) as follows

$$\begin{aligned} I(p,q,r) &= \int_0^\infty\int_0^\infty \ln(xy+px+qy+r)\mathrm{e}^{-x-y}\,\mathrm{d}x\mathrm{d}y - \ln r \\ &= \int_0^{+\infty}\left[\ln(\frac{q}{r}y+1)+\mathrm{e}^{\frac{qy+r}{y+p}}E_1(\frac{qy+r}{y+p})\right]\mathrm{e}^{-y}\,\mathrm{d}y \\ &\approx \mathrm{e}^{\frac{r}{q}}E_1(\frac{r}{q})+\int_0^{+\infty}\sum_{\lambda\in\Lambda}h_\lambda\mathrm{e}^{-k_\lambda\frac{qy+r}{y+p}}\mathrm{e}^{-y}\,\mathrm{d}y \end{aligned} \tag{22}$$

where we used an approximation of $E_1(\cdot)$ in [26]:

$$\mathrm{e}^s E_1(s) = \sum_{\lambda\in\Lambda}h_\lambda\mathrm{e}^{-k_\lambda s}, \tag{23}$$

where $\Lambda = \{\lambda=(u,v)\in\mathbb{N}^2 : 1\leq u\leq\tilde{U}+1, 1\leq v\leq\tilde{V}+1\}$, and

$$h_\lambda = 4\sqrt{2}\pi\phi_u\phi_v\sqrt{\chi_u}, \quad k_\lambda = 1-4\chi_u\chi_v, \quad \lambda=(u,v). \tag{24}$$

Here, parameters $\phi_j = (\theta_j-\theta_{j-1})/\pi \geq 0$, $\chi_j = \frac{1}{2}\frac{\cot(\theta_{j-1})-\cot(\theta_j)}{\theta_j-\theta_{j-1}} \geq 1/2$.

The integrand in the last integral in equation (22) can be estimated by using Taylor series as follows

$$\sum_{\lambda\in\Lambda}h_\lambda\mathrm{e}^{-k_\lambda\frac{qy+r}{y+p}}\mathrm{e}^{-y} \approx \sum_{\lambda\in\Lambda}h_\lambda\mathrm{e}^{-k_\lambda q}\sum_{v=0}^{V}\frac{k_\lambda^v(pq-r)^v}{v!(y+p)^v}\mathrm{e}^{-y}. \tag{25}$$

Equation (3.353.2) in [27] proves (18), and hence the theorem. □

4. Outage Probability Analysis

Define $A_{i,j} = \{\text{SINR}_{i,j} \geq \gamma_{\text{th}j}\}$, where $\gamma_{\text{th}j}$ is the target threshold at jth user. Then event $A_{i,j}^c$ means the ith user cannot decode the jth user's signal. An outage event occurs at ith user when any of $A_{i,j}^c$ occurs. In other words, the OP at ith user can be expressed as

$$\mathcal{P}_{\text{out}}^i = \Pr\left(\bigcup_{j=1}^{i} A_{i,j}^c\right) = 1 - \Pr(A_{i,1} \cdots A_{i,i}). \tag{26}$$

Theorem 2. *A closed-form expression of the outage probability at user i ($\mathcal{P}_{\text{out}}^i$) can be obtained as*

$$\begin{aligned}\mathcal{P}_{\text{out}}^i = 1 - \frac{N!\beta_{\text{RU}}^{-1}}{(i-1)!(N-i)!}\sum_{s=0}^{i-1} 2\binom{i-1}{s}(-1)^s \mathrm{e}^{-\left(\frac{\Gamma_2\delta_i^\star}{\beta_{\text{SR}}\Gamma_3}+\chi_{i,s}\delta_i^\star\right)} \\ \cdot\sqrt{\frac{\phi_i}{\chi_{i,s}}}K_1\left(2\sqrt{\phi_i\chi_{i,s}}\right),\end{aligned} \tag{27}$$

where $\chi_{i,s}$, ϕ_i, $\delta_i^\star$ are defined in (31) and $K_1(\cdot)$ denotes the 1st-order modified Bessel function of the second kind.

Proof. Applying (15), it is easy to check that $A_{i,j}$ can be rewritten as

$$A_{i,j} = \left\{|\hat{h}_i|^2 \geq \delta_j, |\hat{h}_{\text{SR}}|^2 \geq \frac{(\Gamma_2|\hat{h}_i|^2 + \Gamma_4)\delta_j}{\Gamma_3(|\hat{h}_i|^2 - \delta_j)}\right\}, \tag{28}$$

where $\delta_j := \frac{\gamma_{\text{th}j}\Gamma_3}{\Gamma_1(\alpha a_j - b_j\gamma_{\text{th}j})}$. By noting that $\delta_j/(|\hat{h}_i|^2 - \delta_j)$ is monotone in δ_j, we arrive at the following result, that is,

$$A_{i,1}\cdots A_{i,i} = \left\{|\hat{h}_i|^2 \geq \delta_i^\star, |\hat{h}_{\text{SR}}|^2 \geq \frac{(\Gamma_2|\hat{h}_i|^2 + \Gamma_4)\delta_i^\star}{\Gamma_3(|\hat{h}_i|^2 - \delta_i^\star)}\right\}, \tag{29}$$

where $\delta_i^\star = \max(\delta_1, \cdots, \delta_i)$. Now, by (19) and (26),

$$\begin{aligned}\mathcal{P}_{\text{out}}^i &= 1 - \Pr(A_{i,1}\cdots A_{i,i}) \\ &= 1 - \int_{\delta_i^\star}^{\infty} f_i(y)\int_{\frac{(\Gamma_2 y+\Gamma_4)\delta_i^\star}{\Gamma_3(y-\delta_i^\star)}}^{\infty} \mathrm{d}F_{|\hat{h}_{\text{SR}}|^2}(x)\mathrm{d}y \\ &= 1 - \frac{N!\beta_{\text{RU}}^{-1}\mathrm{e}^{-\frac{\Gamma_2\delta_i^\star}{\beta_{\text{SR}}\Gamma_3}}}{(i-1)!(N-i)!}\sum_{s=0}^{i-1}\binom{i-1}{s}(-)^s\int_{\delta_i^\star}^{\infty}\mathrm{e}^{-\left(\chi_{i,s}y+\frac{\phi_i}{y-\delta_i^\star}\right)}\mathrm{d}y,\end{aligned} \tag{30}$$

where

$$\chi_{i,s} = \frac{N-i+s+1}{\beta_{\text{RU}}}, \quad \phi_i = \frac{\delta_i^\star(\Gamma_4 + \delta_i^\star\Gamma_2)}{\beta_{\text{SR}}\Gamma_3}. \tag{31}$$

It follows from (3.471.9) in [27] that (27) holds, and hence the theorem. □

5. Numerical Results

In the numerical parts, we discuss the impact of the following parameter changes on the system performance: different transmission power(SNR) at the first and second phase, different loop back interference levels, different channel estimation error levels and different quantization bits of the ADCs.

Fig. 3 and 4 plots the outage probability and ergodic rate versus SNR at first phase(γ_1) with $cee = 0.001$, $\beta_{\text{LI}} = 0.005$, $\beta_{\text{SR}} = 0.4$, $\beta_{\text{RU}} = 0.6$, $\gamma_2 = 20$dB, quantization bits= 6, power allocation coefficients= $[\frac{1}{2}, \frac{1}{3}, \frac{1}{6}]$ and $\gamma_{\text{th}} = [0.1, 0.1, 0.1]$dB. Fig. 5 and 6 plots the

outage probability and ergodic rate versus SNR at second phase(γ_2) with $cee = 0.001$, $\beta_{\mathrm{LI}} = 0.005$, $\beta_{\mathrm{SR}} = 0.4$, $\beta_{\mathrm{RU}} = 0.6$, $\gamma_1 = 30$dB, quantization bits= 6, power allocation coefficients= $[\frac{1}{2}, \frac{1}{3}, \frac{1}{6}]$ and $\gamma_{\mathrm{th}} = [0.1, 0.1, 0.1]$dB. Fig. 7 and 8 plots the outage probability and ergodic rate versus different loop back interference levels (β_{LI}) with $cee = 0.001$, $\beta_{\mathrm{SR}} = 0.4$, $\beta_{\mathrm{RU}} = 0.6$, $\gamma_1 = 30$dB, $\gamma_2 = 20$dB, quantization bits= 6, power allocation coefficients= $[\frac{1}{2}, \frac{1}{3}, \frac{1}{6}]$ and $\gamma_{\mathrm{th}} = [0.1, 0.1, 0.1]$dB. Fig. 9 and 10 versus lots the outage probability and ergodic rate versus different channel estimation error level and quantization bits with $\beta_{\mathrm{LI}} = 0.005$, $\beta_{\mathrm{SR}} = 0.4$, $\beta_{\mathrm{RU}} = 0.6$, $\gamma_1 = 30$dB, $\gamma_2 = 20$dB, and power allocation coefficients= $[\frac{1}{2}, \frac{1}{3}, \frac{1}{6}]$.

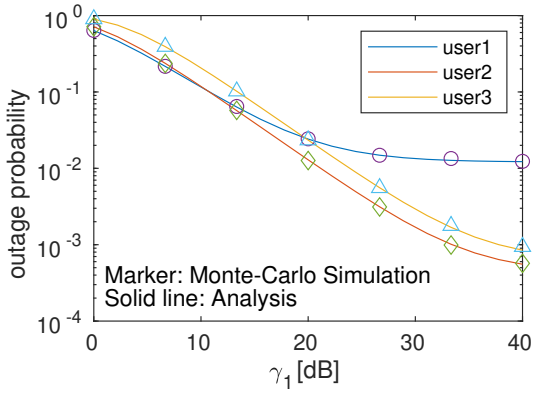

Figure 3. Outage probability versus SNR at first phase(γ_1) with $cee = 0.001$, $\beta_{\mathrm{LI}} = 0.005$, $\beta_{\mathrm{SR}} = 0.4$, $\beta_{\mathrm{RU}} = 0.6$, $\gamma_2 = 20$dB, quantization bits= 6, power allocation coefficients= $[\frac{1}{2}, \frac{1}{3}, \frac{1}{6}]$ and $\gamma_{\mathrm{th}} = [0.1, 0.1, 0.1]$dB.

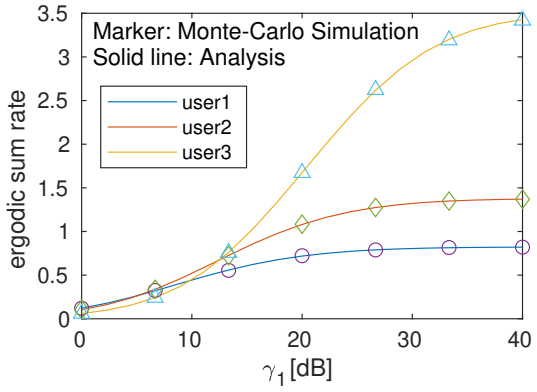

Figure 4. Ergodic rates versus SNR at first phase(γ_1) with $cee = 0.001$, $\beta_{\mathrm{LI}} = 0.005$, $\beta_{\mathrm{SR}} = 0.4$, $\beta_{\mathrm{RU}} = 0.6$, $\gamma_2 = 20$dB, quantization bits= 6, and power allocation coefficients= $[\frac{1}{2}, \frac{1}{3}, \frac{1}{6}]$.

We see here that the greater the transmit power of the first-stage transmission, the lower the outage probability of the system and the higher the ergodic rate. This is also intuitively consistent. When the transmit power of the first stage is fixed, the outage probability and the ergodic rate of the second stage transmit power are also compared. It can be seen that when the SNR of the second stage is about 20dB, the average outage probability of the system is the lowest. However, in the process of increasing the SNR of the second-stage transmission, the outage probability of the system first decreases, and the ergodic rate first increases. However, after a certain stage, continuing to increase the second-stage transmit power will only make the system performance becomes worse. This is because continuing to increase the transmit power of the second stage will introduce a larger power of loopback self-interference, and the loopback self-interference masks the

signal of the system itself, which increase the outage probability and decrease of ergodic capacity, that is the performance deteriorates.

In the figure where the signal-to-noise ratio and channel estimation error are fixed, and the level of loopback self-interference elimination is discussed, it can be seen that the loopback self-interference has a malignant effect on the ergodic rate and outage probability of each user. From zero to after a certain amount of loopback self-interference, the performance of the system quickly becomes poor. Therefore, better self-interference cancellation is required in the communication system of a full-duplex relay. It should be considered that proper RF domain self-jamming cancellation, analog domain self-jamming cancellation, and digital domain self-jamming cancellation need to be considered on relays. The more incomplete the loopback self-interference is the higher the system interruption probability and the lower the ergodic channel capacity. In addition, the relationship between each interruption probability and the transmission signal-to-noise ratio in this chapter does not show a waterfall effect. That is, the interruption probability of the system has no "threshold value" effect, and the change of the interruption probability is relatively gentle in the process of gradually increasing the transmission signal-to-noise ratio.

When the channel estimation error level is $1/1000$, the channel coefficient variances of the first stage and the second stage are 0.4 and 0.6 respectively, the number of quantization bits is 6, and the self-interference level of the loopback is $6/1000$. The outage probability and ergodic channel capacity of the three users tend to be saturated after the transmission signal-to-noise ratio in the first stage reaches 30dB. Since the user with the best channel condition in the NOMA protocol will be assigned the smallest power coefficient, the first user has the highest interruption probability and the lowest ergodic rate.

Finally, in the joint comparison between the channel estimation error level and the number of quantization bits of the analog-to-digital converter, it can be seen that the average outage probability and ergodic rate of the system after the number of quantization bits reaches 6, further increasing the number of quantization bits brings little performance gain/ The level of channel estimation error at this time is more important to the system performance than the quantization bits of the ADC. This suggests that we can reduce the part of the analog-to-digital converter in the system cost and increase the accuracy of the channel estimation.

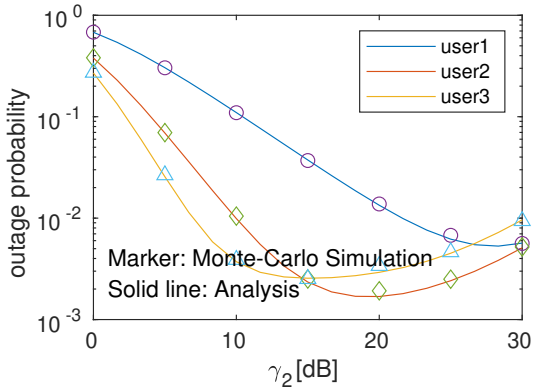

Figure 5. Outage probability versus SNR at second phase(γ_2) with $cee = 0.001$, $\beta_{\mathrm{LI}} = 0.005$, $\beta_{\mathrm{SR}} = 0.4$, $\beta_{\mathrm{RU}} = 0.6$, $\gamma_1 = 30$dB, quantization bits= 6, power allocation coefficients= $[\frac{1}{2}, \frac{1}{3}, \frac{1}{6}]$ and $\gamma_{\mathrm{th}} = [0.1, 0.1, 0.1]$dB.

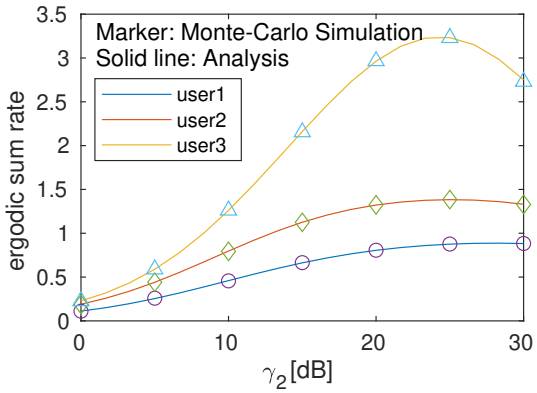

Figure 6. Ergodic rates versus SNR at second phase(γ_2) with $cee = 0.001$, $\beta_{\mathrm{LI}} = 0.005$, $\beta_{\mathrm{SR}} = 0.4$, $\beta_{\mathrm{RU}} = 0.6$, $\gamma_1 = 30$dB, quantization bits= 6, and power allocation coefficients= $[\frac{1}{2}, \frac{1}{3}, \frac{1}{6}]$.

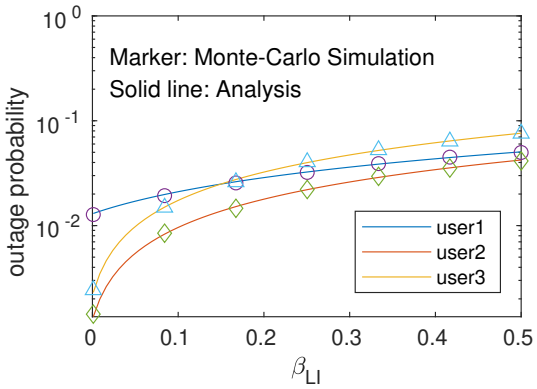

Figure 7. Outage probability versus different loop back interference levels (β_{LI}) with $cee = 0.001$, $\beta_{\mathrm{SR}} = 0.4$, $\beta_{\mathrm{RU}} = 0.6$, $\gamma_1 = 30$dB, $\gamma_2 = 20$dB, quantization bits= 6, power allocation coefficients= $[\frac{1}{2}, \frac{1}{3}, \frac{1}{6}]$ and $\gamma_{\mathrm{th}} = [0.1, 0.1, 0.1]$dB.

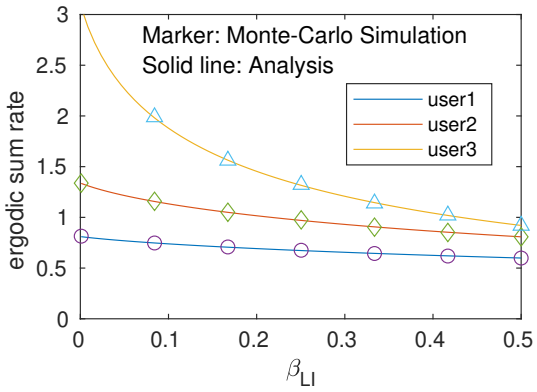

Figure 8. Ergodic rates versus different loop back interference levels (β_{LI}) with $cee = 0.001$, $\beta_{\mathrm{SR}} = 0.4$, $\beta_{\mathrm{RU}} = 0.6$, $\gamma_1 = 30$dB, $\gamma_2 = 20$dB, quantization bits= 6, and power allocation coefficients= $[\frac{1}{2}, \frac{1}{3}, \frac{1}{6}]$.

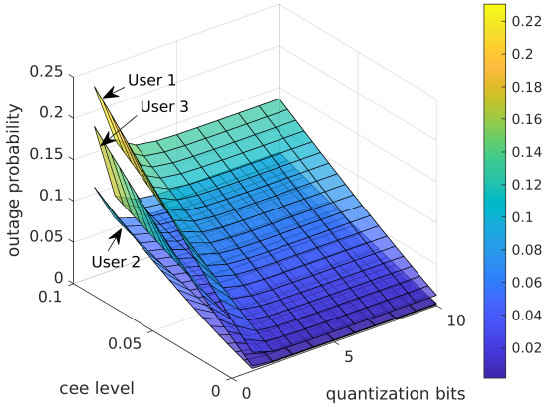

Figure 9. Outage probability versus channel estimation error level and quantization bits with $\beta_{\mathrm{LI}} = 0.005$, $\beta_{\mathrm{SR}} = 0.4$, $\beta_{\mathrm{RU}} = 0.6$, $\gamma_1 = 30\mathrm{dB}$, $\gamma_2 = 20\mathrm{dB}$, power allocation coefficients$= [\frac{1}{2}, \frac{1}{3}, \frac{1}{6}]$, $\gamma_{\mathrm{th}} = [0.1, 0.1, 0.1]\mathrm{dB}$.

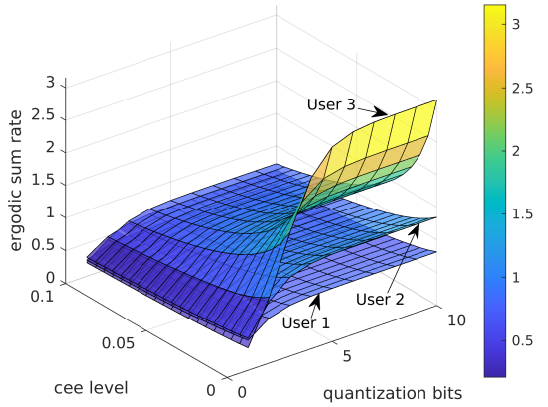

Figure 10. Ergodic rates versus different channel estimation error level and quantization bits with $\beta_{\mathrm{LI}} = 0.005$, $\beta_{\mathrm{SR}} = 0.4$, $\beta_{\mathrm{RU}} = 0.6$, $\gamma_1 = 30\mathrm{dB}$, $\gamma_2 = 20\mathrm{dB}$, and power allocation coefficients$= [\frac{1}{2}, \frac{1}{3}, \frac{1}{6}]$.

6. Conclusion

In this paper, the outage probability and ergodic rates of the full-duplex cooperative NOMA system are analyzed and evaluated in the presence of channel estimation errors and low-resolution ADCs by deriving a closed-form expression for the outage probability and an approximate expression for the ergodic rates for each user. Our results show that the performance is strongly degraded by transmitting signal-to-noise ratio at base station and the relay. Meanwhile, the performance is also influenced by the loop back interference level, channel estimation accuracy and the quantization bits in ADCs. Finally, the accuracy of each formula we derived was assessed by Monte-Carlo simulations.

Author Contributions: investigation, methodology and supervision: Siye Wang; simulation and validation, Yeqin Huang; conceptualization and formal analysis, Yong Yang; writing—original draft preparation and visualization, Yeqin Huang and Yong Yang; writing—review and editing, Siye Wang. All authors have read and agreed to the published version of the manuscript.

Funding: This research received no external funding.

Institutional Review Board Statement: Not applicable.

Data Availability Statement: The source files are free under a BSD license . Our data and matlab codes can be found at https://bupt-yy.github.io/notes/Miscellaneous.

Acknowledgments: The authors would like to thank a referee for several insightful comments and suggestions which helped us to improved the paper.

Conflicts of Interest: The authors declare that they have no conflict of interests.

Abbreviations

The following abbreviations are used in this manuscript:

ADCs	Analog to Digital Converters
AF	Amplify-and-forward
BER	Bit Error Rate
BS	Base Station
cdf	cumulative (probability measure) distribution function
CDMA	Code-Division Multiple Access
CSI	Channel State Information
CNOMA	Cooperative NOMA
ch.f.	Characteristic Function
CSI	channel state information
DF	Decode-and-forward
ER	Ergodic Rate
FD	Full-duplex
FDMA	Frequency-Division Multiple Access
HD	Half-duplex
IBFD	In-band Full-duplex
i.i.d.	Independent and Identically Distributed
LI	Loopback interference
NOMA	Non-Orthogonal Multiple Access
OFDMA	Orthogonal Frequency-Division Multiple Access
OMA	Orthogonal Multiple Access
OP	Outage Probability
Qos	Quality of Service
pdf	Probability Density Function
RF	Radio Frequency
r.v.	Random Variable
SER	Symbol Error Rate
SIC	Successive Interference Cancellation
SINR	Signal-to-interference-plus-noise ratio
SNR	Signal-to-noise Ratio
TDMA	Time-Division Multiple Access
UE	User Equipment

References

1. Ding, Z.; Liu, Y.; Choi, J.; Sun, Q.; Elkashlan, M.; Chih-Lin, I.; Poor, H.V. Application of non-orthogonal multiple access in LTE and 5G networks. *IEEE Commun. Mag.* **2017**, *55*, 185–191.
2. Dai, L.; Wang, B.; Ding, Z.; Wang, Z.; Chen, S.; Hanzo, L. A survey of non-orthogonal multiple access for 5G. *IEEE Commun. Surveys Tuts.* **2018**, *20*, 2294–2323.
3. Men, J.; Ge, J. Non-orthogonal multiple access for multiple-antenna relaying networks. *IEEE Commun. Lett.* **2015**, *19*, 1686–1689.
4. So, J.; Sung, Y. Improving non-orthogonal multiple access by forming relaying broadcast channels. *IEEE Commun. Lett.* **2016**, *20*, 1816–1819.
5. Lva, L.; Chen, J.; Ni, Q.; Ding, Z. Design of cooperative nonorthogonal multicast cognitive multiple access for 5G systems: User scheduling and performance analysis. *IEEE Trans. Commun.* **2017**, *65*, 2641–2656.
6. Choi, J.I.; Jain, M.; Srinivasan, K.; Levis, P.; Katti, S. Achieving single channel, full duplex wireless communication. In Proceedings of the Proc. 16th Annu. Int. Conf. Mobile Comput. Netw., 2010, pp. 1–12.
7. Duarte, M.; Dick, C.; Sabharwal, A. Experiment-driven characterization of full-duplex wireless Systems. *IEEE Trans. Wireless Commun.* **2012**, *11*, 4296–4307.

8. Duarte, M.; Sabharwal, A. Full-duplex wireless communications using off-the-shelf radios: Feasibility and first results. In Proceedings of the Proc. 44th Asilomar Conference on Signals, Systems and Computers, 2010, pp. 1558–1562.
9. Korpi, D.; Tamminen, J.; Turunen, M.; Huusari, T.; Choi, Y.; Anttila, L.; Talwar, S.; Valkama, M. Full-Duplex Mobile Device: Pushing the Limits. *IEEE Commun. Mag.* **2016**, pp. 80–87.
10. Zhang, Z.; Ma, Z.; Xiao, M.; Ding, Z.; Fan, P. Full-duplex device-todevice-aided cooperative nonorthogonal multiple access. *IEEE Trans. Veh. Technol.* **2017**, *66*, 4467–4471.
11. Zhong, C.; Zhang, Z. Non-orthogonal multiple access with cooperative full-duplex relaying. *IEEE Commun. Lett.* **2016**, *20*, 2478–2481.
12. Zhang, L.; Liu, J.; Xiao, M.; Wu, G.; Liang, Y.C.; Li, S. Performance analysis and optimization in downlink NOMA systems with cooperative full-duplex relaying. *IEEE J. Sel. Areas Commun.* **2017**, *35*, 2398–2412.
13. Wang, X.; Jia, M.; Ho, I.W.H.; Guo, Q.; Lau, F.C.M. Exploiting Full-Duplex Two-Way Relay Cooperative Non-Orthogonal Multiple Access. *IEEE Trans. Commun.* **2019**, *67*, 2478–2481.
14. Liu, Y.; Zhang, S.; Mu, X.; Ding, Z.; Schober, R.; Al-Dhahir, N.; Hossain, E.; Shen, X. Evolution of NOMA Toward Next Generation Multiple Access (NGMA) for 6G. *IEEE Journal on Selected Areas in Communications* **2022**, *40*, 1037–1071. doi:10.1109/JSAC.2022.3145234.
15. Patel, S.; Chauhan, D.; Gupta, S. An Overview of Non Orthogonal Multiple Access for Future Radio Communication. In Proceedings of the 2021 International Conference on Intelligent Technologies (CONIT), 2021, pp. 1–3. doi:10.1109/CONIT51480.2021.9498336.
16. Li, X.; Liu, M.; Deng, C.; Mathiopoulos, P.T.; Ding, Z.; Liu, Y. Full-Duplex Cooperative NOMA Relaying Systems With I/Q Imbalance and Imperfect SIC. *IEEE Wireless Communications Letters* **2020**, *9*, 17–20. doi:10.1109/LWC.2019.2939309.
17. Kim, J.B.; Lee, I.H. Capacity Analysis of Cooperative Relaying Systems Using Non-Orthogonal Multiple Access. *IEEE Communications Letters* **2015**, *19*, 1949–1952. doi:10.1109/LCOMM.2015.2472414.
18. Kong, C.; Zhong, C.; Jin, S.; Yang, S.; Lin, H.; Zhang, Z. Full-Duplex Massive MIMO Relaying Systems With Low-Resolution ADCs. *IEEE Trans. on Wireless Commun.* **2017**, *16*, 5033–5047.
19. Wang, D.; Wang, S. Outage Performance for full-duplex decode-and-forward relay Cooperative Networks with low-resolution ADCs. In Proceedings of the 2018 IEEE/CIC International Conference on Communications in China (ICCC); , 2018.
20. Jiao, R.; Dai, L.; Zhang, J.; MacKenzie, R.; Hao, M. On the Performance of NOMA-Based Cooperative Relaying Systems Over Rician Fading Channels. *IEEE Trans. Veh. Technol.* **2017**, *66*, 11409–11413.
21. Liu, Z.; Zhang, L.; Ding, Z. Overcoming the Channel Estimation Barrier in Massive MIMO Communication via Deep Learning. *IEEE Wireless Communications* **2020**, *27*, 104–111. doi:10.1109/MWC.001.1900413.
22. Babu, V.S.; Deepan, N.; Rebekka, B. Performance Analysis of Cooperative Full Duplex NOMA system in Cognitive Radio Networks. In Proceedings of the 2020 International Conference on Wireless Communications Signal Processing and Networking (WiSPNET), 2020, pp. 84–87. doi:10.1109/WiSPNET48689.2020.9198341.
23. Deepan, N.; Rebekka, B. Outage Performance of Full duplex Cooperative NOMA with Energy harvesting over Nakagami-m fading channels. In Proceedings of the 2019 TEQIP III Sponsored International Conference on Microwave Integrated Circuits, Photonics and Wireless Networks (IMICPW), 2019, pp. 435–439. doi:10.1109/IMICPW.2019.8933186.
24. Aswathi, V.; A. V., B. Outage and Throughput Analysis of Full-Duplex Cooperative NOMA System With Energy Harvesting. *IEEE Transactions on Vehicular Technology* **2021**, *70*, 11648–11664. doi:10.1109/TVT.2021.3112596.
25. Devore, J.L.; Berk, K.N.; Carlton, M.A. *Modern mathematical statistics with applications*; Vol. 285, Springer, 2012.
26. Alkheir, A.; Ibnkahla, M. An accurate approximation of the exponential integral function using a sum of exponentials. *IEEE Commun. Lett.* **2013**, *17*, 1364–1367.
27. I.S.Gradshteyn.; Ryzhik, I. Table of Integrals, Series and Products. In Proceedings of the 8th ed.; , 2014.